Pol. J. Environ. Stud. Vol. XX, No. X (XXXX), 1-9
DOI: *10.15244/pjoes/204428* ONLINE PUBLICATION DATE: 2025-07-03

Original Research

Mechanism of Air Purification Combined with Photocatalysis for Controlling Mercury Pollution in Vegetable Greenhouses

Shuxia Gui, Rongguo Sun°*

Guizhou Normal University, Guiyang 550001, PR China

Received: 15 February 2025
Accepted: 27 April 2025

Abstract

Vegetable greenhouses, as semi-enclosed systems, exhibit unique mercury (Hg) dynamics due to elevated temperatures, which enhance Hg(0) volatilization from the soil, leading to atmospheric Hg(0) accumulation. This poses the dual risks of direct crop contamination and secondary pollution through foliar uptake. This study investigates the effects of air purification combined with UV light on atmospheric Hg (GEM) concentration and soil Hg(0) emission flux in a simulated vegetable greenhouse, as well as the underlying mechanisms of Hg migration and transformation. The experimental results show that air purification significantly reduced the GEM concentration in the greenhouse, with a decline rate of over 79% (from 9164.12 ng m^{-3} to 1892.61 ng m^{-3}) within 10 hours. Additionally, it inhibited soil Hg(0) release, with a reduction of over 72% (from 24087.98 ng m^{-2} h^{-1} to 6570.96 ng m^{-2} h^{-1}) in the Hg(0) emission flux. Hydroxyl radicals (·OH) generated by UV photocatalysis promoted Hg(0) oxidation and absorption reactions, significantly enhancing the conversion efficiency of Hg from the gas phase to the liquid phase. Fluid dynamics simulations revealed that air circulation accelerated the optimization of Hg migration pathways and slowed the accumulation of local Hg concentrations. Mass balance analysis indicated that Hg in the greenhouse forms a dynamic equilibrium between soil, gas, and liquid phases, with air purification effectively regulating this process. This study provides scientific evidence and technical support for Hg pollution control in agricultural environments and offers a reference for optimizing greenhouse management and achieving sustainable agricultural development.

Keywords: vegetable greenhouse, mercury pollution, air purification, oxidation absorption, soil mercury emission flux

Introduction

Mercury (Hg), one of the most toxic heavy metals in nature, is highly volatile and persistent [1]. Additionally, it exhibits strong bioaccumulation and biomagnification effects, posing serious health risks to humans through the food chain [2, 3]. In agricultural ecosystems, the accumulation and pollution of Hg have become significant concerns, especially in vegetable greenhouses, which are unique semi-enclosed environments characterized by high temperatures

*e-mail: srg@gznu.edu.cn
°ORCID iD: 0000-0002-8788-5539

and humidity [4]. On one hand, this relatively stable environment promotes rapid crop growth, meeting the human demand for vegetables and fruits [5]. On the other hand, Hg in the soil becomes more volatile under high-temperature conditions [6], and the increased humidity influences the diffusion and deposition of Hg [7], leading to the accumulation of atmospheric Hg(0) (GEM) within the greenhouse, with relatively high concentrations [8]. For instance, a study by Sun et al. found that when the soil Hg concentration was only 0.095 mg kg^{-1} (far below the minimum limit of the Soil Environmental Quality-Risk Control Standard for Soil Contamination of Agricultural Land), the atmospheric Hg(0) concentration inside the greenhouse could reach as high as 102.4 ng m^{-3} [9], which is much higher than the atmospheric Hg(0) concentrations in ordinary farmland (3.26-10.8 ng m^{-3}) [10]. Unfortunately, vegetable leaves can absorb GEM through stomatal respiration and oxidize it into mercuric ion [Hg(II)], which is then fixed in the leaves by coordination with intracellular glutathione and other compounds [11]. This is the predominant pathway for plant leaves to accumulate Hg [12]. Existing studies have confirmed that the excessive atmospheric Hg(0) concentrations in greenhouses caused by Hg(0) release from soil have led to Hg contamination in leaf vegetables such as lettuce, cabbage, and bok choy, thereby threatening regional food safety [13, 14].

Currently, traditional remediation technologies for Hg-contaminated soils primarily include artificial induction or microbial-enhanced phytoremediation, modification of biochar and other novel materials for passivation, electrokinetic remediation, chemical leaching, thermal desorption, and soil amendment techniques [15-19]. These technologies are generally inefficient, or even if they are efficient, they have limitations such as stringent operational conditions, high costs, secondary pollution, damage to soil physical and chemical properties, and even the loss of soil function, making them more suitable for site remediation [20] but not for controlling Hg(0) release in greenhouse soils. Research on control methods for Hg(0) release from greenhouse soils is relatively limited. Liu et al. used iron-modified montmorillonite to control Hg(0) release from greenhouse soils, which showed some effectiveness and allowed the Hg content in vegetables to meet the Tolerance Limit of Hg in Foods (0.01 mg kg^{-1}) (NHCPRC and NMPA, 2017) [4]. Sun et al. found that the application of organic fertilizers in greenhouse soils reduced both Hg(0) emission flux and atmospheric Hg(0) concentration [9]. Although existing research has partially reduced soil Hg(0) emission flux and atmospheric Hg(0) concentrations inside greenhouses, the direct control of atmospheric Hg(0) concentrations in greenhouses remains limited. Therefore, developing a direct, effective, and rapid technique to reduce atmospheric Hg(0) concentrations in vegetable greenhouses is still a critical issue to be addressed. Air purification, a common indoor air pollution control measure [21], may play a positive role in reducing atmospheric Hg(0) concentrations in vegetable greenhouses. However, there is a lack of systematic studies on the effects of air purification operations on Hg migration and transformation mechanisms within greenhouses.

To this end, this study builds a simulated greenhouse and adopts a combined approach of air purification and UV photocatalytic oxidation to explore the effects of air purification operations on atmospheric Hg(0) concentration and soil Hg(0) emission flux in vegetable greenhouses. The aim is to reveal the practical effects of air purification in improving greenhouse air quality and reducing Hg pollution risks, providing scientific support for Hg pollution prevention and control in agricultural production.

Materials and Methods

Experimental Procedure

This study investigates the effects of air purification operations on atmospheric Hg(0) concentration and soil Hg(0) emission flux in a simulated vegetable greenhouse. The simulated greenhouse was constructed with a polypropylene (PP) frame and polyethylene film (with a photosynthetically active radiation (PAR) transmittance of 85% for 400-700 nm), with dimensions of 104 cm × 82 cm × 51 cm. The atmospheric Hg(0) concentration in the empty greenhouse (treatment without soil) is 40.74±0.73 ng m^{-3}. Soil collected from a vegetable greenhouse in Aozhai Township, Wanshan District, Tongren City, Guizhou Province (109.21°E, 27.52°N, altitude: 370 m) was naturally air-dried indoors, ground to 10 mesh (2 mm), and mixed evenly. The soil was then uniformly spread at the bottom of the greenhouse to a thickness of approximately 6 cm. The air purification device was suspended 10 cm above the ground at the center of the greenhouse to simulate air movement (Fig. 1). A control treatment was set up without an air purification device. Both treatments (with and without air purification) were replicated three times, with all greenhouses placed in an open, unobstructed outdoor area. After setting up the greenhouse and air purifier, the purifier was turned on at 9:00 AM on May 31, 2024, to begin the experiment. Atmospheric Hg(0) concentration and soil Hg(0) emission flux were measured immediately after the purifier was turned on (0 hour), as well as at 0.5, 2, 5, 8, and 10 hours to observe the effects of air purification on atmospheric Hg(0) concentration and soil Hg(0) emission flux in the greenhouse.

The air purifier (Fig. 1) consists of a pump, UV light source, and sodium nitrate ($NaNO_3$) absorption solution. Once activated, the purifier draws air from the cylindrical intake tube at the top, with a total airflow rate of 100 L min^{-1}. The UV lamp has a length of 30.2 cm, with a peak emission at 254 nm and a power of 8 W.

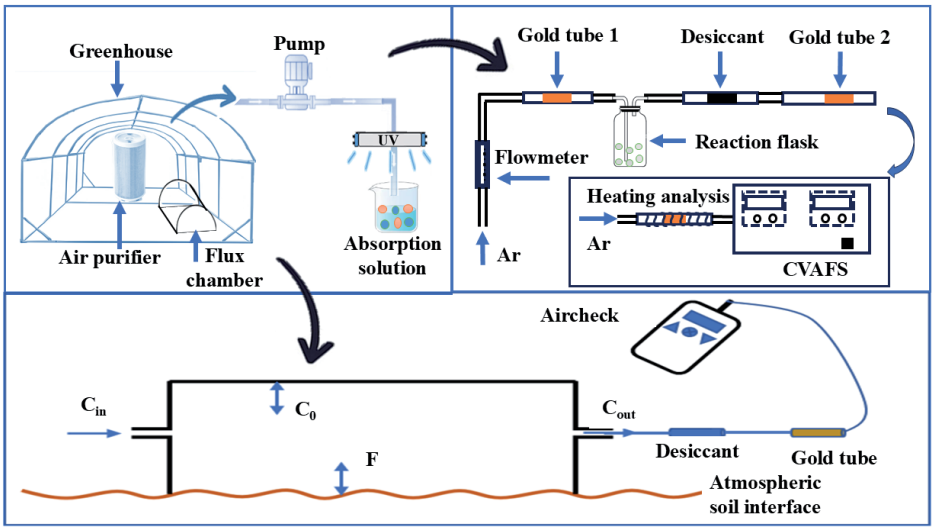

Fig. 1. Experimental summary diagram.

A 300 mL $NaNO_3$ absorption solution (100 mg L^{-1}) is placed 5 cm below the UV lamp. The air pump draws Hg-containing air, which is then bubbled through the sodium nitrate solution at the bottom of the chamber. Under UV light, nitrate ions (NO_3^-) generate hydroxyl radicals (·OH), which oxidize Hg(0) into Hg^{2+}, allowing the capture and enrichment of Hg(0) from the airflow.

Measurement Methods and Data Analysis

The GEM concentration in the simulated vegetable greenhouse was measured using an air sampler (AirCheck XR5000, SKC Inc., USA) in combination with a gold-amalgam trap for enrichment (Fig. 1). Air was collected for 1 minute at a flow rate of 1 L min^{-1} through a small hole (radius 1 cm) located at the top of the greenhouse. The Hg in the gold-amalgam trap was then thermally desorbed (420ºC) and measured using cold vapor atomic fluorescence spectroscopy (CVAFS, Model III, Brooks Rand, USA). The GEM concentration was calculated using Equation (1).

$$\mathrm{Hg}(0) = \frac{m}{t \times Q} \tag{1}$$

where Hg(0) is the GEM concentration (ng m^{-3}), m is the Hg mass (ng) accumulated in the gold-amalgam trap, t is the sampling time (min), and Q is the sampling flow rate (L min^{-1}).

The soil-atmosphere Hg(0) emission flux was measured using the flux chamber method (Fig. 1). A semicircular quartz flux chamber (bottom area: 0.04 m^2, volume: 0.00314 m^3) was placed on the soil surface, and the surrounding soil was used to seal the perimeter of the flux chamber to ensure there were no gaps between the chamber and the soil. As shown in Fig. 1, the flux chamber, desiccant tube, gold tube, and AirCheck XR5000 sampler (SKC Inc., USA) were connected for sampling. After 1 minute of sampling, the desiccant tube was disconnected, and the gold tube was replaced. The Hg(0) concentration in the air outside the flux chamber was then collected for 1 minute. The accumulated Hg(0) in the two gold tubes was analyzed using CVAFS. The soil Hg(0) emission flux was calculated based on the atmospheric Hg(0) concentration in the greenhouse (C_{in}, ng m^{-3}) and the concentration at the flux chamber outlet (C_{out}, ng m^{-3}) Equation (2).

$$F = \frac{(C_{out} - C_{in} - C_0) \cdot Q}{A} \tag{2}$$

where C_0 is the Hg adsorbed or released by the inner wall of the flux chamber (ng m^{-3}), which serves as the blank value; Q is the sampling flow rate (L min^{-1}); A is the bottom area of the flux chamber (m^2); and F is the soil Hg(0) emission flux (ng m^{-2} h^{-1}).

THg in the $NaNO_3$ absorption solution was determined according to the US EPA method 1631 using bromine chloride (GR, Tianjin Kemio Chemical Reagent Co., Ltd.) oxidation, stannous chloride (GR, Tianjin Kemio Chemical Reagent Co., Ltd.) reduction, gold tube enrichment, 420°C thermal desorption, and CVAFS detection method. Soil total mercury was determined via acid digestion (HNO_3-HCl, 1:3 v/v) followed by CVAFS according to US EPA Method 7473 [22]. The THg concentration in the tested soil was 10±0.18 mg kg^{-1}.

Computational fluid dynamics (CFD) simulations were conducted using ANSYS Fluent v21.0. The greenhouse geometry was meshed with tetrahedral elements (mesh size: 0.5 cm), and airflow was modeled using the k-ε turbulence model. Boundary conditions included an air pump inflow (100 L min^{-1}) and atmospheric pressure outlets.

Quality Assurance and Quality Control

All glassware was subjected to a stringent cleaning procedure before use to prevent contamination. The cleaning protocol involved soaking the glassware in a 25% nitric acid solution for 24 hours to remove potential contaminants and impurities. The glassware was then dried at 100ºC for 4 hours to eliminate moisture and residual substances, followed by natural cooling in an Hg-free environment to ensure instrument purity. All personnel wore disposable gloves throughout the experiment and took precautions to avoid cross-contamination. The water used in the experiment was Hg-free ultrapure water with a resistivity of 18.2 MΩ cm^{-1}, ensuring that no Hg contamination was introduced into the experimental setup.

Results and Discussion

Effect of Air Purification on Atmospheric Hg(0) Concentrations in Vegetable Greenhouses

Air purification operations significantly influenced the dynamic variation of GEM concentration in the vegetable greenhouse (Fig. 2). In the experimental group with air purification, GEM concentrations showed a significant downward trend as the purification time increased. The concentration decreased from the initial value of 9164.12 ng m^{-3} to 1892.61 ng m^{-3} after 10 hours, with an overall reduction rate of 79.35%. In contrast, the control group (without air purification) showed fluctuations in GEM concentration (4771.09-7976.17 ng m^{-3}) over time, without a clear downward trend. Moreover, the decline rate in GEM concentration was most significant in the first 2 hours of air purification (more than 67%), after which the decline rate gradually slowed. This may be due to the rapid removal of volatile gaseous Hg(0) in the greenhouse. After that, the Hg(0) release rate from the soil became relatively balanced with the air purification rate, leading to a slower decrease in GEM concentration.

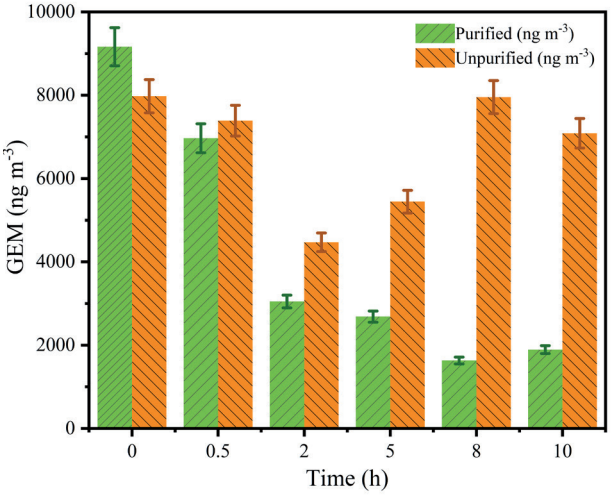

Fig. 2. Variation of GEM concentration over time in the greenhouse with air purification treatment and the control group.

These results indicate that air purification operations significantly reduced the accumulation of gaseous Hg(0) in the greenhouse. Statistical analysis (ANOVA) showed that GEM concentrations at different time points in the experimental group with air purification were significantly lower than those in the control group (two-tailed T test, $P = 0.043$). This validates the effectiveness of the air purification operation, indicating that continuous air purification can effectively reduce Hg pollution in the greenhouse. Therefore, this study provides an effective Hg pollution control method, suggesting that introducing air purification technology in vegetable greenhouses in Hg-polluted areas can significantly reduce the risk of atmospheric Hg(0) pollution and ensure the safety of agricultural products.

Variation of Soil Hg(0) Emission Flux in Vegetable Greenhouses

Air purification operations significantly affected the soil-to-air Hg(0) emission flux (Fig. 3). In the air purification treatment group, the soil Hg(0) emission flux gradually decreased as the purification time increased, from an initial value of 24087.98 ng m^{-2} h^{-1} to 6570.96 ng m^{-2} h^{-1} after 10 hours, representing a reduction of 72.72%. In contrast, the soil Hg(0) emission flux in the control group (12473-19347 ng m^{-2} h^{-1}) remained relatively stable, with only slight fluctuations. This result indicates that air purification operations significantly suppressed the continuous release of Hg(0) from the soil by reducing the greenhouse's atmospheric Hg(0) concentration.

The rate of decline in the soil Hg(0) emission flux in the air purification treatment was most significant during the first 2 hours, after which it gradually leveled off. This could be because the more volatile Hg(0) in the surface soil was released first, while the migration and release of deeper Hg(0) was limited by the diffusion rate. Additionally, the control group reflected the changes in soil Hg(0) emission flux under the influence of light, temperature, and soil physical-chemical properties, further verifying that air purification operations can reduce soil Hg(0) emission flux regardless of external conditions.

Combined with the GEM concentration analysis, the experimental data further confirmed the positive correlation between soil Hg(0) release and atmospheric Hg(0) concentration in the greenhouse ($R^2 = 0.88$). This relationship is mechanistically linked to the regulation of near-ground Hg vapor pressure. By reducing atmospheric Hg(0) levels through air purification, the partial pressure gradient driving Hg(0) volatilization from soil to air is diminished, as described

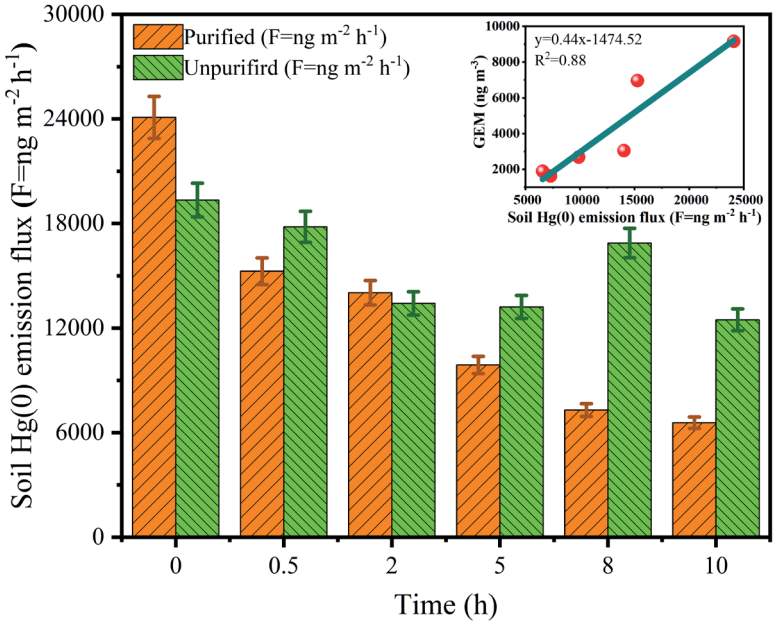

Fig. 3. Variation of soil Hg(0) emission flux over time.

by Henry's law governing gas-liquid equilibrium [23]. Consequently, the lowered near-ground Hg(0) vapor pressure suppresses soil Hg(0) emission flux. Compared to traditional agricultural greenhouse management practices, this study proposes an effective strategy to mitigate soil Hg(0) release by directly targeting the thermodynamic driving force (vapor pressure) through air purification.

Fluid Dynamics Simulation of Airflow in the Greenhouse

Fluid dynamics simulations were conducted to reveal the impact of air purification operations on airflow distribution and flow paths within the vegetable greenhouse (Fig. 4). The simulation results showed that the airflow characteristics inside the greenhouse

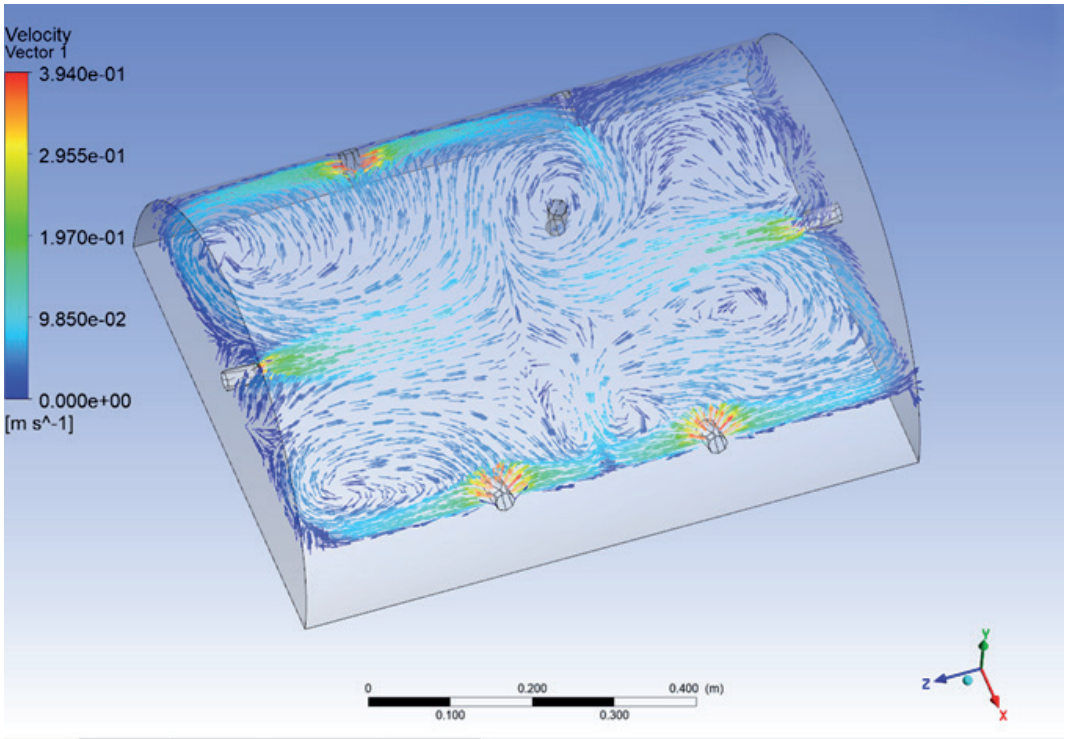

Fig. 4. Simulated airflow velocity contour map in the greenhouse.

underwent significant changes under the influence of air purification operations. The airflow, driven by the circulation effect of the air pump, accelerated the circulation of air inside the greenhouse, reducing the accumulation of gaseous Hg(0) (GEM) in localized areas and significantly improving the overall air uniformity within the greenhouse.

In the experiment, airflow mainly entered through the holes at the top and around the greenhouse and flowed along the inner surfaces of the greenhouse structure, ultimately being discharged from the air pump outlet at the opposite end. This flow path effectively reduced stagnant areas and high-concentration regions of gaseous Hg(0). Meanwhile, a localized airflow separation phenomenon was observed near the inner walls, forming small-scale vortices near the center-lower part of the structure. The presence of these vortices could lead to airflow reattachment, which might reduce the air circulation efficiency in localized regions. However, properly adjusting the air pump flow rate and position can significantly minimize the vortex effect on overall airflow movement.

The simulation results also revealed a distinct gradient in the airflow speed distribution, with faster airflow near the air pump outlet and slower airflow further away. This speed distribution characteristic indicates that the air pump plays a dominant role in the airflow inside the greenhouse and can effectively control the migration path of gaseous Hg(0). To further enhance the air purification efficiency, optimizing the air pump arrangement or adding auxiliary ventilation devices can improve the uniformity and coverage of the airflow.

The fluid dynamics simulations revealed that airflow patterns significantly influence Hg(0) migration pathways. Importantly, the efficacy of air purification is highly dependent on device-specific parameters. Higher flow rates (>150 L min^{-1}) may enhance Hg(0) removal but risk disturbing the soil surface and resuspending particulate-bound Hg, while lower rates (<50 L min^{-1}) may inadequately disrupt near-ground Hg(0) gradients [24]. Positioning the purifier closer to the soil surface (e.g., 5 cm vs. 10 cm) could improve localized Hg(0) capture but may reduce overall airflow uniformity [25]. Our optimized design (100 L min^{-1}, suspended 10 cm above ground) balances efficiency and practicality, suggesting that device parameters must be tailored to specific greenhouse geometries and Hg contamination levels.

Through fluid dynamics simulations, this study quantitatively demonstrates the impact of air purification operations on airflow distribution within vegetable greenhouses for the first time, providing important insights into the migration mechanisms of Hg pollution in greenhouses. This result not only has significant guidance for optimizing greenhouse environmental management but also provides a scientific reference for the design of airflow and ventilation systems in greenhouses.

Oxidation and Absorption of Atmospheric Hg(0)

The experimental results indicate that the combination of air purification operations and UV lamp irradiation significantly affects the oxidation and absorption reactions of Hg in the solution (Fig. 5). Under continuous UV lamp irradiation, the Hg concentration in the absorption solution gradually increased over time, demonstrating the continuous oxidation and absorption of GEM. During the initial stage (0-2 hours), the Hg concentration in the solution increased rapidly, from 17.17 ng L^{-1} to approximately 173.37 ng L^{-1}. After 2 hours, the rate of increase slowed down, and after 10 hours, the Hg concentration approached stability, reaching around 285.14 ng L^{-1}. This phenomenon suggests that the rate of oxidation and absorption of GEM was highest in the initial stage and then gradually slowed down due to limitations in reactant concentration and reaction kinetics.

The UV lamp played a crucial role in the process, as the ultraviolet radiation emitted by the lamp excited nitrate ions (NO_3^-) in the solution to generate highly reactive hydroxyl radicals (·OH) [26]. These radicals rapidly oxidized GEM into divalent Hg (Hg^{2+}), causing the Hg(0) to migrate from the gas phase to the liquid phase. This indicates that photocatalysis directly influences the oxidation and absorption of GEM, with continuous UV irradiation driving the oxidation and absorption reactions toward equilibrium, leading to a stable concentration of Hg^{2+} after a certain period.

When implemented in the greenhouse, the UV lamp's photocatalytic effect effectively enhanced the oxidation and absorption efficiency of Hg, significantly reducing the concentration of gaseous Hg(0) in the greenhouse. This, in turn, indirectly reduced the release pressure of Hg from the soil. These results provide a practical and feasible technological pathway for Hg pollution control in agricultural greenhouses.

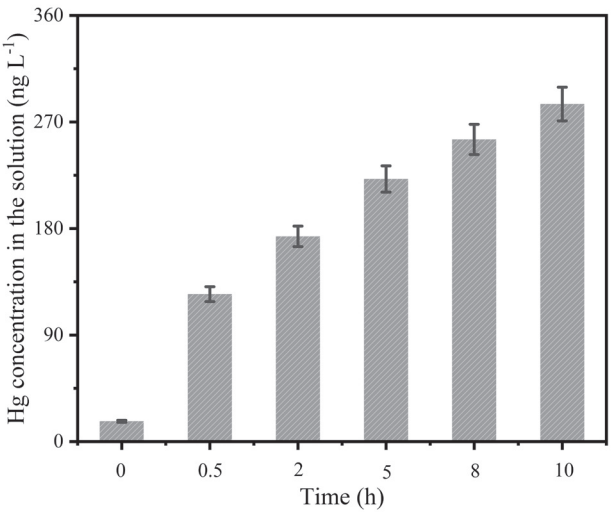

Fig. 5. Hg concentration in the solution.

Under UV lamp irradiation, NO_3^- undergoes a photochemical reaction to generate ·OH radicals, and Equations (3) and (4) can describe the reaction mechanism.

$$NO_3^- + h\nu \rightarrow NO_2^- + O^- \quad (3)$$

$$O^- + H_2O \rightarrow \cdot OH + OH^- \quad (4)$$

The highly reactive ·OH radicals rapidly undergo oxidation reactions with gaseous Hg(0), forming the stable Hg^{2+} form, as shown in the following reaction:

$$Hg^0_{(aq)} + \cdot OH_{(aq)} \rightarrow Hg^+_{(aq)} + OH^-_{(aq)} \quad (5)$$

$$Hg^+_{(aq)} + \cdot OH_{(aq)} \rightarrow Hg^{2+}_{(aq)} + OH^-_{(aq)} \quad (6)$$

The oxidation rate of Hg(0) by ·OH is primarily controlled by Equation (5). By calculating the rate constant (k) for the reaction between hydroxyl radicals and gaseous Hg(0), the dynamic characteristics of this process can be better understood. Literature data indicates that the rate constant for the oxidation of Hg(0) by ·OH is 2.0×10^9 M^{-1} s^{-1}, which is consistent with the increasing trend of Hg concentration in the solution under UV irradiation conditions in this experiment, further validating the efficiency of the oxidation and absorption process [27].

Mass Balance Analysis

This experiment employed mass balance analysis to evaluate the dynamic distribution characteristics of Hg among the soil-air interface release, gas phase, and absorption solution phases within the vegetable greenhouse and to reveal the influence mechanism of air purification operations on Hg migration and transformation (Fig. 6). The results indicate that the migration and release of Hg(0) in the greenhouse follows a dynamic equilibrium pattern. A combination of factors, including airflow circulation, temperature and humidity conditions, and the oxidation-absorption reaction, influences the distribution characteristics.

In the initial stage of the experiment (0 hours), the gaseous Hg(0) (GEM) accounted for approximately 11% of the total Hg, while the soil Hg(0) emission flux contributed 89%, indicating that the primary source of atmospheric Hg(0) in the greenhouse was Hg(0) released from the soil. As the air purification operation progressed, the proportion of GEM gradually decreased, and the proportion of soil Hg(0) emission flux was also significantly reduced. After 10 hours, the GEM proportion dropped to 8%, while the concentration of Hg^{2+} in the solution significantly increased, accounting for nearly 50%. This result indicates that air purification operations, through the air pump extraction and UV lamp irradiation, effectively facilitated the conversion of Hg(0) from the gas phase to the solution phase while inhibiting further release of Hg(0) from the soil.

The mass balance analysis also showed that multiple factors controlled the dynamic changes of Hg in the greenhouse. First, the air purification operation significantly reduced the accumulation of gaseous Hg(0) in the greenhouse, thereby weakening the concentration gradient driving force for soil Hg(0) release. Second, the ·OH generated by UV-driven nitrate photolysis (Equations (3) and (4)) oxidized gaseous Hg(0) through a two-step reaction (Equations (5) and (6)). The resulting Hg^{2+} ions were stabilized in the sodium

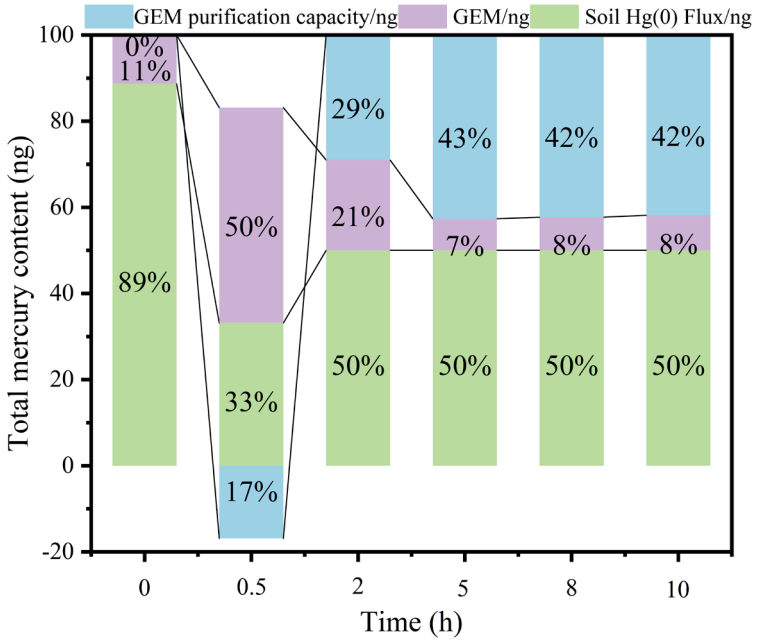

Fig. 6. Mass balance analysis.

nitrate absorption solution via coordination with nitrate ligands ($Hg(NO_3)_2$), effectively enhancing the phase transfer efficiency by converting volatile Hg(0) into non-volatile, water-soluble complexes [28]. These mechanisms worked synergistically to significantly reduce the Hg pollution load in the greenhouse.

The experiment also revealed that the Hg distribution in the greenhouse gradually stabilized over time, indicating that the release, migration, and transformation of Hg reached a dynamic equilibrium state. After 10 hours, changes in soil Hg(0) emission flux and gaseous Hg(0) concentration leveled off, and the concentration of Hg^{2+} in the solution remained high. This dynamic equilibrium may be related to the limited deep diffusion of soil Hg(0) and the constraints of reaction kinetics. Moreover, the enclosed nature of the greenhouse environment further slowed the interference of external Hg pollution sources on the system's equilibrium.

The mass balance analysis in this experiment provides important insights into Hg's migration and transformation mechanisms within the greenhouse. Compared to Hg migration studies in open environments, the semi-enclosed conditions in the greenhouse amplified the effects of air purification operations, significantly enhancing the efficiency of Hg migration and transformation. The experimental results indicate that by reasonably designing the air purification system within the greenhouse, the dynamic distribution of Hg can be effectively controlled, enabling long-term management of Hg pollution in agricultural ecosystems.

In conclusion, air purification operations significantly influence the mass balance of Hg in the greenhouse. The dynamic variation mechanism reflects the synergistic effects of multiple factors, including airflow circulation, temperature and humidity control, and photocatalytic oxidation. This study provides a technical reference for controlling Hg pollution in agricultural greenhouses and lays the scientific foundation for optimizing related environmental management measures.

Conclusions

By constructing a simulated vegetable greenhouse, this study thoroughly investigated the effects of air purification operations on atmospheric Hg(0) concentration, soil Hg(0) emission flux, and Hg oxidation-absorption reactions within the greenhouse. The experimental results show that air purification combined with UV lamp irradiation significantly reduced the concentration of GEM in the greenhouse while also inhibiting Hg release from the soil. Both soil Hg(0) emission flux and atmospheric Hg(0) concentration exhibited a clear downward trend throughout the experiment, eventually reaching a dynamic equilibrium. By accelerating air circulation and optimizing temperature and humidity conditions, this process regulated the migration pathway of Hg within the greenhouse and significantly reduced the risk of Hg pollution accumulation.

Furthermore, the oxidation and absorption of Hg were driven by hydroxyl radicals generated through photocatalysis, greatly enhancing the conversion efficiency of gaseous Hg(0) to the liquid phase. This study reveals, from multiple dimensions, the migration and transformation patterns of Hg within the greenhouse, providing a scientific basis for Hg pollution control in agricultural environments. The results indicate that air purification operations not only reduce Hg pollution in the greenhouse but also effectively improve air quality and ensure the safety of agricultural products. This comprehensive strategy holds broad practical application potential and provides essential support for optimizing greenhouse environmental management and promoting sustainable agricultural development.

Acknowledgments

This study was financially supported by the National Natural Science Foundation of China (No. 42067025 and 42367028) and the Science and Technology Department of Guizhou Province (No. Qian ke he ji chu [2020] 1Z038 and Qian ke he ping tai ren cai-YQK [2023] 027).

Conflict of Interest

The authors declare no conflict of interest.

References

1. DRISCOLL C.T., MASON R.P., CHAN H.M., JACOB D.J., PIRRONE N. Mercury as a Global Pollutant: Sources, Pathways, and Effects. Environmental Science & Technology. **47** (10), 4967, **2013**.
2. PAVITHRA K.G., SUNDARRAJAN P., KUMAR P.S., RANGASAMY G. Mercury sources, contaminations, mercury cycle, detection and treatment techniques: A review. Chemosphere. **312**, 137314, **2023**.
3. ZHU D., HAN J., WU S. The Bioaccumulation and Migration of Inorganic Mercury and Methylmercury in the Rice Plants. Polish Journal of Environmental Studies. **26** (4), 1905, **2017**.
4. LIU C., LONG L., YANG Y., ZHANG Y., WANG J., SUN R. The mechanisms of iron modified montmorillonite in controlling mercury release across mercury-contaminated soil-air interface in greenhouse. Science of the Total Environment. **812**, 152432, **2022**.
5. LIANG Y., JING X., WANG Y., SHI Y., RUAN J. Evaluating Production Process Efficiency of Provincial Greenhouse Vegetables in China Using Data Envelopment Analysis: A Green and Sustainable Perspective. Processes. **7** (11), 780, **2019**.
6. MOORE C.W., CASTRO M.S. Investigation of factors affecting gaseous mercury concentrations in soils. Science of the Total Environment. **419**, 136, **2012**.
7. ZHANG G., ZHOU X., LI X., WANG L., LI X., LUO Z., ZHANG Y., YANG Z., HU R., TANG Z., WANG D.,

WANG Z. Gaseous Elemental Mercury Exchange Fluxes over Air-Soil Interfaces in the Degraded Grasslands of Northeastern China. Biology. **10** (9), 917, **2021**.
8. YU Q., LUO Y., WANG S.X., WANG Z.Q., HAO J.M., DUAN L. Gaseous elemental mercury (GEM) fluxes over canopy of two typical subtropical forests in south China. Atmospheric Chemistry and Physics. **18** (1), 495, **2018**.
9. SUN R., ZHAO T., FAN L., ZHANG Y., WANG J., YANG Y., JIANG T., TONG Y. The transformation of soil Hg oxidation states controls elemental Hg release in the greenhouse with applying organic fertilizer. Journal of Hazardous Materials. **454**, 131520, **2023**.
10. SHI T., GONG Y., MA J., WU H., YANG S., JU T., QU Y., LIU L. Soil-air exchange of mercury from agricultural fields in Zhejiang, East China: Seasonal variations, influence factors, and models of fluxes. Chemosphere. **249**, 126063, **2020**.
11. ZHANG T., LU Q., SU C., YANG Y., XU Q. Mercury induced oxidative stress, DNA damage, and activation of antioxidative system and Hsp70 induction in duckweed (*Lemna minor*). Ecotoxicology and Environmental Safety. **143**, 46, **2017**.
12. BECKERS F., AND RINKLEBE J. Cycling of mercury in the environment: Sources, fate, and human health implications: A review. Critical Reviews in Environmental Science and Technology. **47** (9), 693, **2017**.
13. WAI K.M., DAI J., YU P.K.N., ZHOU X., WONG C.M.S. Public health risk of mercury in China through consumption of vegetables, a modelling study. Environmental Research. **159**, 152, **2017**.
14. XIA J., WANG J., ZHANG L., ANDERSON C.W.N., WANG X., ZHANG H., DAI Z., FENG X. Screening of native low mercury accumulation crops in a mercury-polluted mining region: Agricultural planning to manage mercury risk in farming communities. Journal of Cleaner Production. **262**, 121324, **2020**.
15. KALOGERAKIS N., FAVA F., CORVINI P.F.X. Bioremediation advances. New Biotechnology. **38**, 41, **2017**.
16. KUMAR A., KUMAR V., CHAWLA M., THAKUR M., BHARDWAJ R., WANG J., O'CONNOR D., HOU D., RINKLEBE J. Bioremediation of mercury contaminated soil and water: A review. Land Degradation & Development. **35** (4), 1261, **2024**.
17. WANG Y., RUI D., NIE W., KIM M., HU D., ZHANG J., LIU J. Remediation of Pb- and, Cd-contaminated soil through magnetic-modified eluent synergetic freeze-thaw and washing. Cold Regions Science and Technology. **216**, 104000, **2023**.
18. AZHAR A.T.S., NABILA A.T.A., NURSHUHAILA M.S., ZAIDI E., AZIM M.A.M., FARHANA S.M.S. Assessment and Comparison of Electrokinetic and Electrokinetic-bioremediation Techniques for Mercury Contaminated Soil. IOP Conference Series: Materials Science and Engineering. **160** (1), 012077, **2016**.
19. NAVARRO A., CAÑADAS I., MARTINEZ D., RODRIGUEZ J., MENDOZA J.L. Application of solar thermal desorption to remediation of mercury-contaminated soils. Solar Energy. **83** (8), 1405, **2009**.
20. XU J., BRAVO A.G., LAGERKVIST A., BERTILSSON S., SJöBLOM R., KUMPIENE J. Sources and remediation techniques for mercury contaminated soil. Environment International. **74**, 42, **2015**.
21. COLLINS D.B., FARMER D.K. Unintended Consequences of Air Cleaning Chemistry. Environmental Science & Technology. **55** (18), 12172, **2021**.
22. LOWERY T.A., WINTERS R.S., GARRETT III E.S. Comparison of Total Mercury Determinations of Fish Fillet Homogenates by Thermal Decomposition, Amalgamation, and Atomic Absorption Spectrophotometry versus Cold Vapor Atomic Absorption Spectrophotometry. Journal of Aquatic Food Product Technology. **16** (2), 5, **2007**.
23. CARRERO J.I. Beyond Henry's law in the gas–liquid equilibrium. ChemTexts. **8** (1), 1, **2021**.
24. KIM M.Y., JUNG Y.G., PARK J.C., YANG Y.K. The impact of airflow and air purification on the resuspension and removal of deposited particulate matter. Journal of Building Engineering. **41**, 102367, **2021**.
25. ZHANG Y., KACIRA M., AN L. A CFD study on improving air flow uniformity in indoor plant factory system. Biosystems Engineering. **147**, 193, **2016**.
26. ZHANG Y., SUN R., MA M., WANG D. Study of inhibition mechanism of NO_3^- on photoreduction of Hg(II) in artificial water. Chemosphere. **87** (2), 171, **2012**.
27. ZHANG H. Photochemical Redox Reactions of Mercury. Recent Developments in Mercury Science. In: Atwood, D.A. (eds)., Springer: Berlin, Heidelberg, Germany. **120**, 37, **2006**.
28. SI L., ARIYA P.A. Recent Advances in Atmospheric Chemistry of Mercury. Atmosphere. **9** (2), 76, **2018**.